

# The Impact of $\gamma$ -Irradiation and EtO Degassing on Tissue Remodeling of Collagen-based Hybrid Tubular Templates

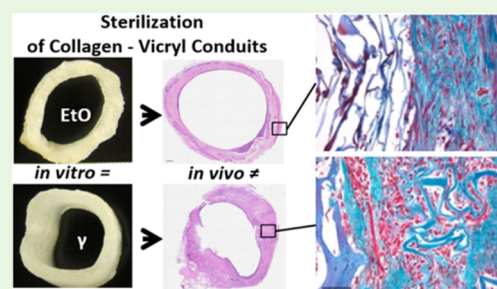
Marije Sloff,<sup>†,§,#</sup> Heinz P. Janke,<sup>†,#</sup> Paul K. J. D. de Jonge,<sup>†,||</sup> Dorien M. Tiemessen,<sup>†</sup> Barbara B. M. Kortmann,<sup>†,‡</sup> Silvia M. Mihaila,<sup>†,⊥</sup> Paul J. Geutjes,<sup>†</sup> Wout F. J. Feitz,<sup>†,‡,#</sup> and Egbert Oosterwijk<sup>\*,†,#</sup>

<sup>†</sup>Department of Urology, Radboud Institute for Molecular Life Sciences, Radboud University Medical Center, Geert Grooteplein 28 Zuid, 6525 GA Nijmegen, The Netherlands

<sup>‡</sup>Radboudumc Amalia Children's Hospital, Radboud University Medical Center, Geert Grooteplein 10 Zuid, 6525 GA Nijmegen, The Netherlands

**ABSTRACT:** Clinical implementation of novel products for tissue engineering and regenerative medicine requires a validated sterilization method. In this study, we investigated the effect of  $\gamma$ -irradiation and EtO degassing on material characteristics *in vitro* and the effect on template remodeling of hybrid tubular constructs in a large animal model. Hybrid tubular templates were prepared from type I collagen and Vicryl polymers and sterilized by 25 kGray of  $\gamma$ -irradiation or EtO degassing. The *in vitro* characteristics were extensively studied, including tensile strength analysis and degradation studies. For *in vivo* evaluation, constructs were subcutaneously implanted in goats for 1 month to form vascularized neo-tissue. Macroscopic and microscopic appearances of the  $\gamma$ - and EtO-sterilized constructs slightly differed due to additional processing required for the COL-Vicryl-EtO constructs. Regardless of the sterilization method, incubation in urine resulted in fast degradation of the Vicryl polymer and decreased strength (<7 days). Incubation in SBF was less invasive, and strength was maintained for at least 14 days. The difference between the two sterilization methods was otherwise limited. In contrast, subcutaneous implantation showed that the effect of sterilization was considerable. A well-vascularized tube was formed in both cases, but the  $\gamma$ -irradiated construct showed an organized architecture of vasculature and was mechanically more comparable to the native ureter. Moreover, the  $\gamma$ -irradiated construct showed advanced tissue remodeling as shown by enhanced ECM production. This study shows that the effect of sterilization on tissue remodeling cannot be predicted by *in vitro* analyses alone. Thus, validated sterilization methods should be incorporated early in the development of tissue engineered products, and this requires both *in vitro* and *in vivo* analyses.

**KEYWORDS:** collagen type I, polyglactin 910 (Vicryl), sterilization, animal model (goat), tensile strength, tissue remodeling



## INTRODUCTION

Recent advances in the field of tissue engineering and regenerative medicine have led to the application of advanced tissue engineered products (skin grafts, tracheas, cartilage, bladder augmentations) in different patient groups, albeit patient numbers were limited.<sup>1–4</sup> The majority of research within this field is still at the preclinical stage, and novel biomaterials are still being developed for a variety of indications. Evaluation of novel biomaterials varies from mechanical characterization and degradation studies to cyto- and biocompatibility assays.<sup>5,6</sup> In general, the first step in *in vivo* evaluation is limited to subcutaneous implantation in small animals.<sup>7,8</sup> For evaluation in larger animals, and in particular for successful clinical translation and implementation, standardized production with medical grade materials is required. One of the essential steps in this process is sterilization of constructs using a validated sterilization procedure.<sup>9</sup> The choice of sterilization method may affect the mechanical and biological features, for instance due to the aggressiveness of the

sterilization procedure.<sup>10</sup> It is therefore important to evaluate the final sterilized medical grade products *in vitro* and *in vivo*.<sup>11,12</sup>

For preclinical application of biomaterials, gamma( $\gamma$ )-irradiation and ethylene oxide degassing (EtO) are the most frequently used sterilization methods.<sup>13</sup> With  $\gamma$ -irradiation, wet materials can be sterilized, which eliminates additional processing. Materials can therefore be packaged in ethanol, which is necessary for long-term sterility and storage at  $-80$  °C. However, during  $\gamma$ -irradiation of wet materials, free radicals are formed, leading to altered material properties.<sup>9</sup> Ethylene oxide (EtO) is a highly diffusive alkylating agent, and adequate degassing is needed to permit diffusion of remaining toxic derivatives, like chlorohydrin and ethylene glycol.<sup>14</sup> Compared to  $\gamma$ -irradiation, EtO degassing is a less invasive sterilization

Received: March 27, 2018

Accepted: July 25, 2018

Published: July 25, 2018

technique, and this may result in a material with prolonged strength and support. It may therefore be a preferred technique for polymeric materials.<sup>15,16</sup>

Collagen-based templates have been used for various reconstructive purposes, including in preclinical studies for urological tissue engineering to reconstruct parts of the urological tract.<sup>17–19</sup> In a previous study, a  $\gamma$ -irradiated hybrid tubular construct from type I collagen and a biodegradable Vicryl polymer mesh was used to create an artificial urinary conduit in a porcine model.<sup>20</sup> Interestingly, a functional conduit with urinary flow could be created after subcutaneous preimplantation, although severe shrinkage of the graft and skin contraction was observed. The implanted material was completely remodeled and did not provide sufficient structural integrity to prevent contraction. This could have been the consequence of several important aspects. It is possible that urine can contribute to the tissue remodeling as it creates an aberrant (micro)environment which may ultimately lead to deposition of more fibroblasts, leading to graft shrinkage. Second, young (porcine) animals were used, known for their fast growth, specific skin properties, and regeneration.<sup>21</sup> This may also cause excessive wound contraction. Third, the choice of sterilization technique may have extensively influenced the final outcome since  $\gamma$ -sterilization enhances Vicryl biodegradability from 2 months to less than 1 month.<sup>22</sup>

We hypothesized that using a less invasive sterilization technique, i.e., EtO degassing, would result in prolonged template stability and improved remodeling. In this study, we therefore compared two validated sterilization techniques, i.e.,  $\gamma$ -irradiation and EtO degassing, in terms of mechanical properties, degradation, and template remodeling in an adult animal model (goat) mimicking tissue regeneration in the adult patient population.

## MATERIALS AND METHODS

**Tubular Hybrid Template Preparation.** Tubular hybrid templates ( $l = 10$  cm,  $\varnothing = \pm 15$  mm) were prepared in a cleanroom facility (EMCM B.V., Nijmegen, The Netherlands), using a previously described protocol.<sup>23</sup> In brief, a 0.7% (w/v) collagen type I suspension prepared from bovine achilles tendon (Collagen Solutions, Eden Prairie, USA) was combined with a tailor-made tubularized Vicryl polymer mesh (VM74, Ethicon, Somerville, NJ, USA) in a silicon mold. A stainless steel mandrel ( $\varnothing = 15$  mm) was inserted to create a lumen in the tubular construct. After freezing and freeze-drying, scaffolds were strengthened by chemical cross-linking using EDC/NHS.<sup>24</sup> Subsequently, constructs were either packaged in blisters with 70% ethanol for sterilization by a standard dose of 25 kGray of gamma ( $\gamma$ )-irradiation (Synergy Health, Etten-Leur, The Netherlands) or further processed for sterilization by ethylene oxide degassing (EtO, Synergy Health, Venlo, The Netherlands). This required additional freezing and freeze-drying and subsequent packaging in blisters. Cross-linking efficiency was determined by trinitrobenzenesulfonic acid assay,<sup>24</sup> and construct morphology was assessed by scanning electron microscopy (SEM, JEOL 6310) and histology by hematoxylin (Klinipath, Duiven, The Netherlands) and eosin (Boom, Meppel, The Netherlands; HE).

**Tensile Strength Analysis.** The mechanical characteristics of the wetted tubular constructs were evaluated using a tensile tester with a 2.5 kN load cell (Z2.5 TN, Zwick/Roell, Ulm, Germany). A circular ring test was performed on ring pieces of the constructs (width ( $w$ ): 6.4  $\pm$  0.7 mm, thickness ( $t$ ): 3.1  $\pm$  0.4 mm,  $n = 14$  from 2 COL-Vicryl-EtO constructs and  $l$ : 6.1  $\pm$  0.6 mm,  $t$ : 2.9  $\pm$  0.4 mm,  $n = 11$  from 2 COL-Vicryl- $\gamma$  constructs). The hooks of the apparatus were placed in contact with the upper and lower areas opposite each other (hook-to-hook distance), spaced 18.45 mm apart for the COL-Vicryl-EtO and 22.53 mm for the COL-Vicryl- $\gamma$ , avoiding any “prestretch.”

The upper hook was then moved upward with a crosshead speed of 50 mm/min until rupture. Samples were compared to native goat ureters, the primary anastomosis site for the artificial urostomy, which acts as an extended ureter. Ureters from two different goats were similarly analyzed, spaced 1.27 mm apart ( $n = 12$ ). Data generation was performed as previously described.<sup>25,26</sup> In brief, recorded force–displacement data were normalized to the test specimen dimensions to compute a stress–strain curve. The stress was expressed as the recorded force  $F$  [N], which reacted on the cross-sectional area  $A$  [mm<sup>2</sup>] of the test specimen (thickness ( $t$ )  $\times$  width ( $w$ )  $\times$  2), while the strain was expressed as the change in length  $\Delta L$  [mm] divided by its original length (hook-to-hook distance)  $L_0$  [mm]. As an indicator for construct stiffness, the Young's modulus was calculated from the slope (upswing region) of the computed stress–strain curve. Ultimate tensile strength (UTS) and failure strain were defined as the maximum stress and maximum strain, respectively, in the stress–strain curve before failure of the construct.

**Degradation Assay.** A degradation assay was performed in goat urine as well as in simulated body fluid (SBF) over 28 days. The goat urine was centrifuged at 2000g for 10 min at 4 °C and filter sterilized to avoid cellular contaminants and ensure sterility. Urine was kept at 4 °C until use. SBF was created as described.<sup>27</sup> In brief, SBF was made in a plastic beaker with 700 mL of demi-water and the consecutive addition of the following: 9.23 mM NaCl (Merck, Darmstadt, Germany), 0.56 mM NaHCO<sub>3</sub> (Sigma-Aldrich, St. Louis, MO, USA), 0.41 mM Na<sub>2</sub>CO<sub>3</sub> (Boom, Meppel, The Netherlands), 0.30 mM KCl (Sigma-Aldrich, St. Louis, MO, USA), 0.10 mM K<sub>2</sub>HPO<sub>4</sub>·3H<sub>2</sub>O (Merck, Darmstadt, Germany), 0.15 mM MgCl<sub>2</sub>·6H<sub>2</sub>O (Merck, Darmstadt, Germany), 200 mL of 0.2 M NaOH (Merck, Darmstadt, Germany), 7.51 mM HEPES (Invitrogen, Thermo Scientific, Waltham, MA, USA), 0.26 mM CaCl<sub>2</sub> (Sigma-Aldrich, St. Louis, MO, USA), and 0.05 mM Na<sub>2</sub>SO<sub>4</sub> (Sigma-Aldrich, St. Louis, MO, USA). The mixture was then warmed to 36.5 °C and adjusted to pH 7.4 with 1.0 M NaOH (Merck, Darmstadt, Germany). The precipitation potential of the SBF was checked on broken glass at 37 °C. In contrast, the mixture should not precipitate at 4 °C on plastic. Ring pieces of COL-Vicryl-EtO ( $w$ , 6.2  $\pm$  0.8 mm;  $t$ , 2.8  $\pm$  0.5 mm;  $n = 36$  from three constructs) and COL-Vicryl- $\gamma$  ( $w$ , 5.2  $\pm$  0.6 mm;  $t$ , 3.2  $\pm$  0.4 mm;  $n = 36$  from three constructs) were incubated in six-well plates (Corning, Corning, New York, USA) at 37 °C.  $N = 3$  was used for each time point (day 0, 3, 7, 14, and 28) for three different conditions (goat urine and SBF). The constructs were evaluated by histology and tensile strength analysis as described above. COL-Vicryl-EtO and COL-Vicryl- $\gamma$  rings in urine were spaced “hook-to-hook” 21.05  $\pm$  1.75 mm and 21.81  $\pm$  0.40 mm apart, respectively. COL-Vicryl-EtO and COL-Vicryl- $\gamma$  rings in SBF were spaced 24.84  $\pm$  1.50 mm and 21.63  $\pm$  1.27 mm apart, respectively.

**Subcutaneous Implantation.** The animal experiment was approved by the Ethical Committee on Animal Research of the Radboud University Medical Center, Nijmegen, The Netherlands (RU-DEC 2014 233). We included nine adult Saane goats (2–3 years,  $\pm 60$  kg), receiving a restricted diet and water ad libitum. Animals were transported with a “buddy” goat but were individually housed with nose contact after surgery and placed in groups when possible at the animal farm. Randomization and blinding were not possible due to clear differences in physical appearances. Subcutaneous implantation was performed to form vascularized neo-tissue as previously described.<sup>20</sup> Under general anesthesia, subcutaneous pockets were created on the right flank below the muscle layer of the skin, through a 5 cm incision above the shoulder of the right hind leg. In three animals, one COL-Vicryl-EtO construct was preimplanted, and in three other animals, both the COL-Vicryl-EtO and COL-Vicryl- $\gamma$  were implanted in different pockets on the same flank. The pockets were spatially apart to avoid interference of regeneration and/or inflammation. Constructs were extensively washed in PBS, slid over a silicon mandrel, and attached to the mandrel using CT-1 Vicryl sutures (Ethicon, Somerville, NJ, USA). The construct was then inserted into the pocket and attached to the fascia with CT-1 Vicryl sutures (Ethicon). The skin incision was subsequently closed with 2–0 Vicryl (Ethicon) for the subcutaneous



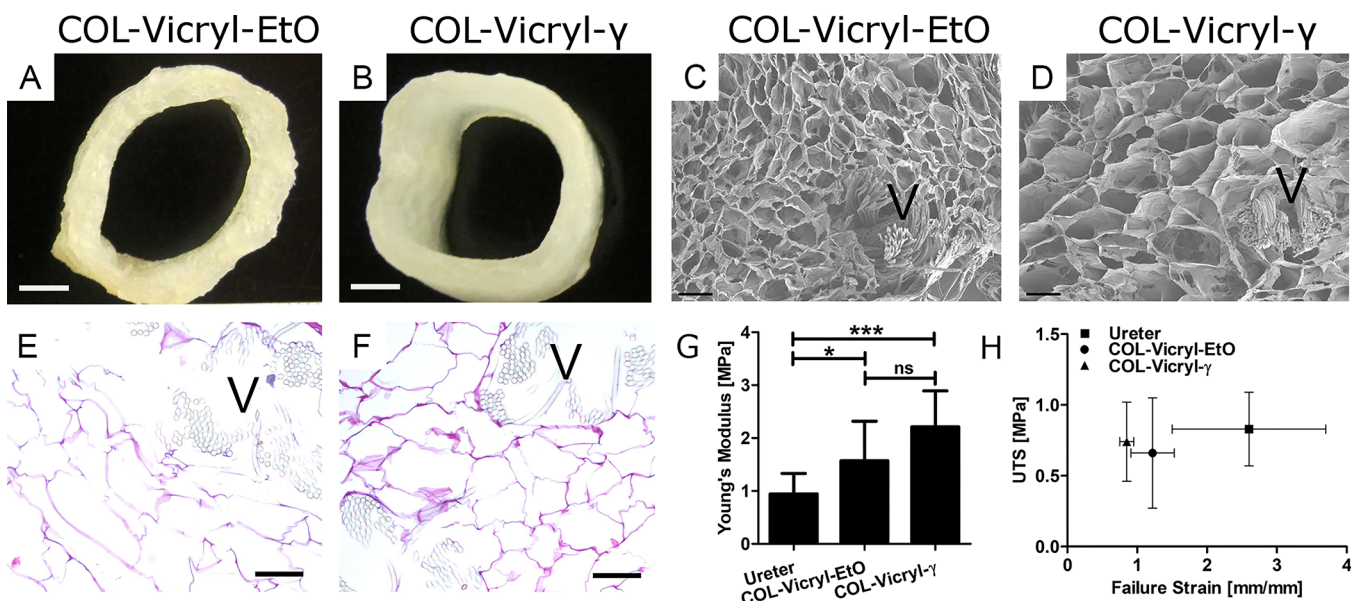


**Figure 1.** Construct analysis. (A,B) Macroscopic overview of the COL-Vicryl-EtO and COL-Vicryl- $\gamma$ , scale bar = 0.5 cm. (C,D) SEM images, scale bar = 250  $\mu$ m, pore size for COL-Vicryl-EtO is approximately 150–250  $\mu$ m and for COL-Vicryl- $\gamma$  200–300  $\mu$ m. (E,F) Histological overview of the construct, scale bar = 250  $\mu$ m. (G,H) Mechanical characteristics of the constructs. V = Vicryl polymer, \* $p < 0.05$ , \*\*\* $p < 0.0001$ , ns = nonsignificant.

fat and the skin. Goats received 15 mg/kg Albipen LA (ampicillin) I.M. during surgery and 15 mg/kg Albipen LA S.C. every 48 h after surgery.

**Evaluation of Implants.** One month later, the remodeled tubes were harvested and evaluated. Ring pieces ( $w$ ,  $7.0 \pm 2.1$  mm;  $t$ ,  $3.1 \pm 0.1$  mm;  $n = 7$  for COL-Vicryl-EtO from two goats and  $w$ ,  $7.0 \pm 1.5$  mm;  $t$ ,  $3.4 \pm 1.0$  mm;  $n = 11$  for COL-Vicryl- $\gamma$  from three goats) were transferred to PBS and immediately measured by tensile strength analysis as described above. The hook spacing was  $12.7 \pm 1.9$  mm for COL-Vicryl-EtO and  $15.5 \pm 0.6$  mm for COL-Vicryl- $\gamma$ , respectively. Ring pieces were transferred to 4% (v/v) formaldehyde (Sigma-Aldrich, St. Louis, MO, USA) in PBS for fixation and subsequent embedding in paraffin for microscopic analysis. HE slides were scored by three independent observers (MS, PG, PdJ) for collagen and Vicryl degradation, inflammation, tissue integration, and vascularity. Averages of the independent scorings were calculated and combined into a scoring profile. Representative slides were used for confirmation by Masson's Trichrome and immunohistochemistry.

**Immunohistochemistry.** Expression of type IV collagen (COLIV) and HIF1 $\alpha$  was analyzed on paraffin-embedded material (5  $\mu$ m thickness), mounted on silane-coated slides (New Silane III, Muto Pure Chemicals Co., Ltd., Tokyo, Japan). After deparaffinization and PBS washings, endogenous peroxidase activity was blocked by incubation in 1% (v/v) H<sub>2</sub>O<sub>2</sub> in PBS for 20 min.

For COLIV, antigen retrieval was performed using 0.05% (v/v) proteinase in PBS (20 min, 37  $^{\circ}$ C, Merck, Darmstadt, Germany). Slides were then washed with PBS/Tween and incubated with 10% (v/v) swine serum (30 min) followed by incubation with the primary antibody (1 h, rabbit- $\alpha$ -human COLIV, 1:250, Abcam, Cambridge, UK). After washings, the sections were incubated with peroxidase-labeled swine- $\alpha$ -rabbit secondary antibody (30 min, SWARPO, 1:100, DakoCytomation, Glostrup, Denmark) followed by washings.

For HIF1 $\alpha$ , heat-induced antigen retrieval was performed using sodium citrate (pH 6) followed by TBS/0.1% Tween20 washings. Blocking of endogenous biotin (and receptors) and avidin receptors (10 min, Vector Laboratories, Burlingame, California, USA) was performed with washing in between. After additional washing, endogenous proteins were blocked with 2% BSA (5 min), directly followed by incubation with the primary antibody (45 min, mouse- $\alpha$ -human HIF1 $\alpha$ , 1:500, BD Biosciences, San Jose, CA, USA). After washings, sections were incubated with a biotin-labeled secondary

antibody (15 min, donkey- $\alpha$ -mouse, 1:500, Jackson ImmunoResearch, West Grove, PA, USA). Slides were then washed and incubated 15 min with peroxidase-labeled streptavidin/biotin complex (1:100 Avidin solution and 1:100 Biotin solution, 30 min preincubation, Vector Laboratories, Burlingame, California, USA). An amplification step was performed after washings using biotinyl tyramide (15 min, DAKO, Heverle, Belgium). After washings, slides were incubated with peroxidase-labeled streptavidin (15 min, 1:250, ThermoScientific, Rockford, IL, USA) followed by washings.

For both COLIV and HIF1 $\alpha$ , sections were developed with Bright-DAB (ImmunoLogic, Duiven, The Netherlands) and counterstained with hematoxylin (Klinipath, Duiven, The Netherlands). For negative controls, the primary antibody was omitted, and no staining was observed in these samples. Native tissue was used for a positive control, showing staining in expected tissue components.

**Statistics.** Data are presented as means with standard deviation and analyzed with Prism software (version 5.03, Graphpad Software Inc., La Jolla, CA, USA). A one-way ANOVA with Bonferroni post hoc test was performed for statistical analysis of differences between COL-Vicryl-EtO, COL-Vicryl- $\gamma$ , and native goat ureter.

## RESULTS

**Construct Analysis.** The macroscopic appearance of the COL-Vicryl-EtO and COL-Vicryl- $\gamma$  constructs can be seen in Figure 1A,B. The luminal diameter ( $13.1 \pm 1.1$  mm for COL-Vicryl-EtO and  $14.6 \pm 1.4$  mm COL-Vicryl- $\gamma$ , respectively) slightly differed due to additional processing (freezing and freeze-drying) required for COL-Vicryl-EtO constructs. Microscopic analysis by scanning electron microscopy and histology showed integration of the Vicryl polymer as indicated by visible collagen–Vicryl connections and a typical honeycomb structure (Figure 1C,D). For the COL-Vicryl-EtO constructs, which required additional processing (freezing and freeze-drying), a thinner and compressed wall with smaller pores was observed (Figure 1E,F). Cross-linking was successful, as indicated by the decrease in free amine groups, and was comparable for both groups: 35% for the COL-Vicryl- $\gamma$  (reduced to  $109 \pm 15$  nmol/mg) and 37% for the COL-Vicryl-EtO (reduced to  $202 \pm 5$  nmol/mg). The mechanical

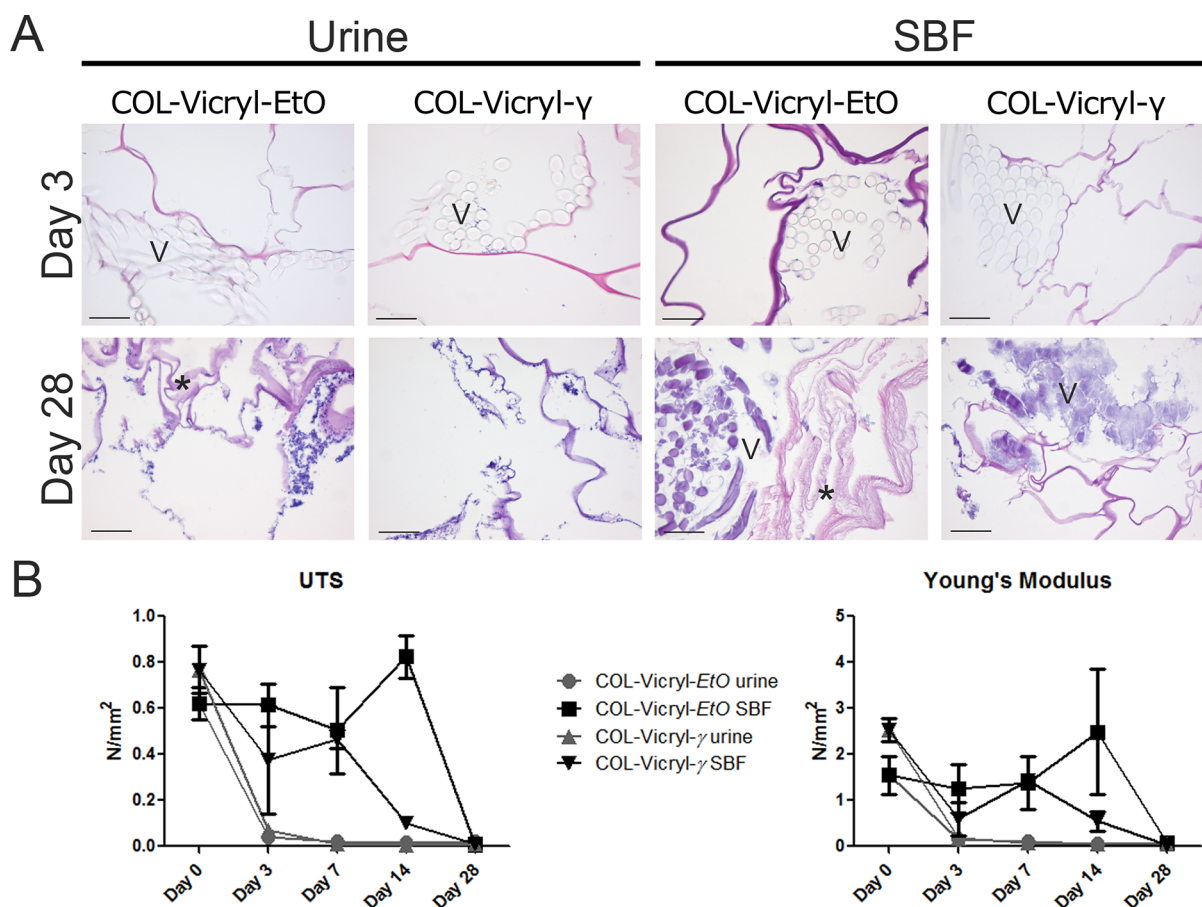


**Figure 2.** Degradation assay. (A) Microscopic overview by HE of the degradation assay in urine and SBF, scale bar = 100  $\mu\text{m}$ , V = Vicryl polymer, \* = collagen degradation. Images presented for urine day 28 are representative for days 14 and 7. Images presented for SBF day 3 are representative for days 7 and 14. (B) Mechanical characteristics of the degraded constructs. Urine exposure resulted in immediate diminished mechanical properties of both construct types at day 3, although the Vicryl was still morphologically visible. In SBF, prolonged mechanical stability was observed until day 14 for both constructs. At day 28, the mechanical properties were lost, and the polymer showed signs of severe degradation.

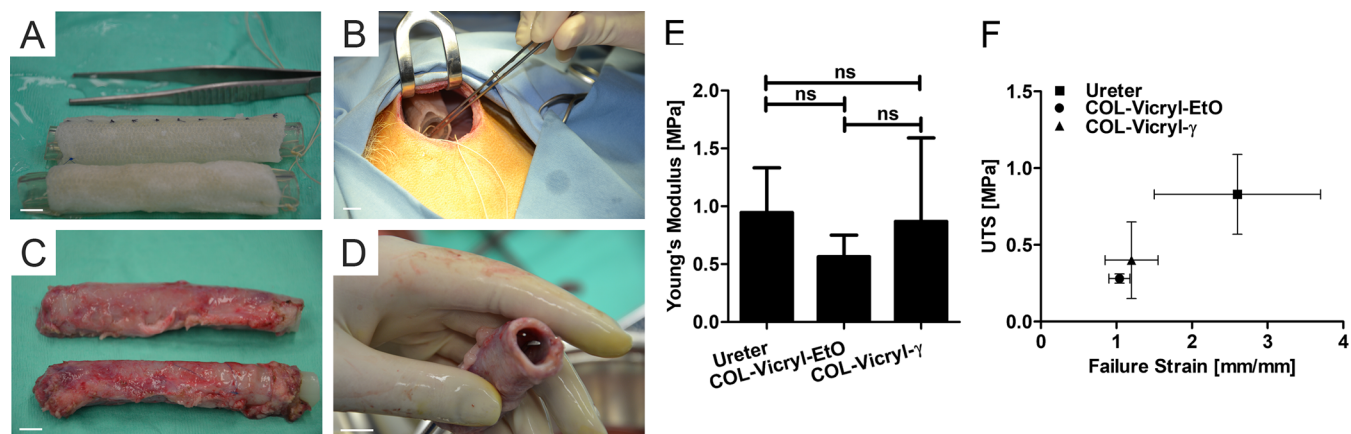


**Figure 3.** Subcutaneous implantation. (A) Overview of the washed constructs with the inserted mandrel, all scale bars 1 cm. COL-Vicryl- $\gamma$  is the upper construct; COL-Vicryl-EtO is the lower construct. (B) Subcutaneous pocket. (C) Autologous tissue tubes one month after implantation (same formation as in A). (D) Open lumen after removal of the mandrel. (E,F) Mechanical characteristics of the implanted constructs compared to native goat ureter. ns = nonsignificant.

characteristics of the construct were compared to native goat ureter, the primary anastomosis site for the construct in an artificial urostomy, and conform the animal model (Figure 1G,H). The COL-Vicryl- $\gamma$  Young's modulus ( $2.31 \pm 0.67$  MPa) was approximately twice as high as that of the ureter ( $0.95 \pm 0.39$  MPa), while the COL-Vicryl-EtO showed a

Young's modulus only 1.5 $\times$  as high ( $1.57 \pm 0.75$  MPa). The ultimate tensile strength (UTS) and failure strain of the ureter and both constructs was similar (ureter,  $0.83 \pm 0.26$  MPa at  $2.6 \pm 1.1$  mm/mm strain; COL-Vicryl-EtO,  $0.66 \pm 0.39$  MPa at  $1.22 \pm 0.31$  mm/mm strain; COL-Vicryl- $\gamma$ ,  $0.74 \pm 0.28$  MPa at  $0.85 \pm 0.10$  mm/mm strain).



**Degradation Assay.** Incubation in goat urine resulted in fast degradation (<7 days) of the Vicryl polymer in both constructs (Figure 2A). Microscopic analysis revealed negative imprints of the multifilamented Vicryl in the scaffold after 3 days. The collagen structure was barely affected in the COL-Vicryl- $\gamma$  constructs. In contrast, swelling of collagen lamellae was seen in the urine-incubated COL-Vicryl-EtO constructs at day 28 (Figure 2A). Tensile strength analysis of the ring pieces showed a strongly diminished UTS and Young's modulus, already after 3 days (Figure 2B), regardless of the sterilization method.

The effect of SBF was less extensive, and Vicryl remnants were still present at 28 days in both constructs, although their original multifilamented structure was lost. Only in the COL-Vicryl-EtO construct was the collagen substantially affected by SBF and showed swelling of collagen lamellae at 14 and 28 days. The UTS and Young's modulus of the constructs in SBF were maintained for at least 14 days. At this evaluation point, COL-Vicryl-EtO showed higher UTS and Young's moduli than COL-Vicryl- $\gamma$ , but after 28 days UTS and Young's moduli of both constructs were similar.

**Subcutaneous Implantation.** Subcutaneous implantation was successful in all goats and for all constructs. After one month, a remodeled neo-tissue tube was formed regardless of the sterilization method. The neo-tissue tube was encapsulated but easy to harvest from the subcutaneous pocket (Figure 3A–D). The rims of the neo-tissue, where scaffold material was absent, were fragile and ruptured easily and were therefore eliminated from analysis. After removal of the mandrel, the firm tissue was able to maintain an open lumen and was suitable for translocation to serve as an artificial urostomy. No clear macroscopic differences between the construct types were observed.

Ring pieces of both implants were analyzed by tensile strength analysis and compared to the native goat ureter (Figure 3E,F). After subcutaneous implantation, the UTS of the COL-Vicryl-EtO was  $0.28 \pm 0.03$  MPa at  $1.04 \pm 0.14$  mm/mm strain and  $0.40 \pm 0.25$  MPa at  $1.26 \pm 0.33$  mm/mm strain for the COL-Vicryl- $\gamma$ . This was significantly lower than the UTS for the native goat ureter ( $0.83 \pm 0.26$  MPa at  $2.6 \pm 1.1$  mm/mm strain). The Young's modulus was similar for all groups (ureter,  $0.95 \pm 0.39$  MPa; COL-Vicryl-EtO,  $0.56 \pm 0.19$  MPa; and COL-Vicryl- $\gamma$ ,  $0.87 \pm 0.72$  MPa). The UTS and Young's modulus of the COL-Vicryl- $\gamma$  implant approximated the native ureter (the tissue to be mimicked in the urostomy) more closely than the COL-Vicryl-EtO.

**(Immuno)Histological Analysis of Implants.** Detailed microscopic evaluation showed a clear difference between the COL-Vicryl-EtO and the COL-Vicryl- $\gamma$  implants (Figure 4 and Table 1). The implanted COL-Vicryl- $\gamma$  constructs were well integrated in the surrounding tissue, and both collagen and the Vicryl polymer were partially degraded. Ingrowing fibroblast-like cells from the surrounding tissue were present within the honeycomb structures of the collagen and between the Vicryl filaments. In contrast, the COL-Vicryl-EtO constructs did not successfully integrate in the surrounding tissue, resulting in a clear boundary between the construct and surrounding tissue in some areas (Figure 4D). Degradation of collagen and Vicryl was substantially less in the COL-Vicryl-EtO constructs. In these less degraded areas of the COL-Vicryl-EtO constructs, increased expression of HIF1 $\alpha$ <sup>+</sup> was observed, indicating hypoxia. Although the amount of vascularity was comparable between groups, a different vascular architecture was observed

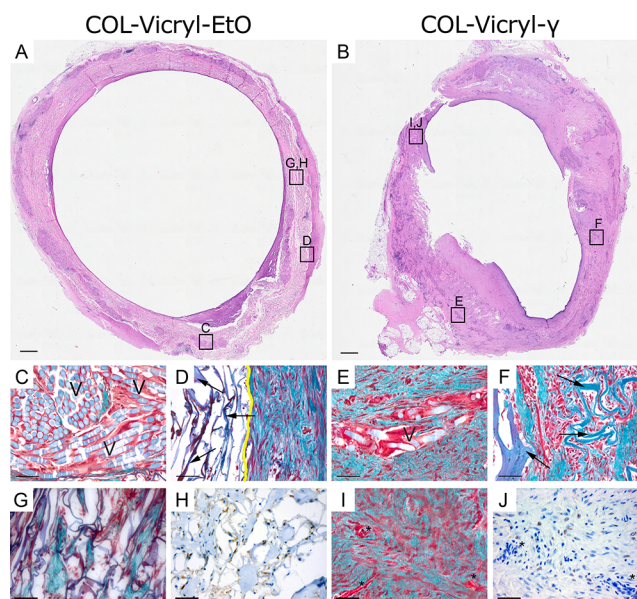


**Figure 4.** Histological and immunohistochemical analysis of the implants. (A,B) Macroscopic overview of ring pieces of COL-Vicryl-EtO and COL-Vicryl- $\gamma$  by HE, scale bar = 1 mm. (C–G, I) Masson's Trichrome staining from indicated boxes in A and B, blue/green = collagen, collagen from constructs is indicated by arrows; light blue (V) = Vicryl polymer; red/brown = cell nuclei; yellow line = construct/tissue boundary; scale bar = 100  $\mu$ m. (G,H) Construct material showing limited regeneration, without vascular structures, but high expression of HIF1 $\alpha$ . (I,J) Construct material showing progressive regeneration with the presence of vascular structures (\*) and limited HIF1 $\alpha$  expression. Scale bar = 200  $\mu$ m.

**Table 1. Scoring Profile<sup>a</sup>**

	Col-Vicryl-EtO	Col-Vicryl- $\Gamma$
collagen degradation	+	++
vicryl degradation	+/-	+
inflammation	+	+
tissue integration	+	++
vasculature	+	+

<sup>a</sup>Hematoxyline and Eosin (HE) slides of implanted COL-Vicryl-EtO and COL-Vicryl- $\gamma$  constructs were independently scored for relative comparison to one another to create a representative profile for each implanted construct. No reference material was used. Items were scored – (not present), +/- (sporadically present), + (moderately present), ++ (abundantly present), or +++ (excessively present).

in the luminal area (Table 1 and Figure 5). In the COL-Vicryl- $\gamma$ , an organized layer of COLIV<sup>+</sup> vasculature was formed, while in the COL-Vicryl-EtO group, an aberrant architecture of vasculature was observed when compared to the vascular bed in normal tissue. Since COL IV staining completely coincided with capillaries, COL IV staining was judged to be an appropriate surrogate marker for the capillary network.

## DISCUSSION

Clinical implementation of biomaterials requires sterilization with EMA (European Medicines Agency) and FDA (United States Food and Drug Administration) -approved techniques, like  $\gamma$ -irradiation or EtO degassing. In the preclinical phase, materials are generally tested *in vitro* and *in vivo* with nonvalidated, in-house disinfection or sterilization methods, to evaluate strength and cyto- and biocompatibility. This study

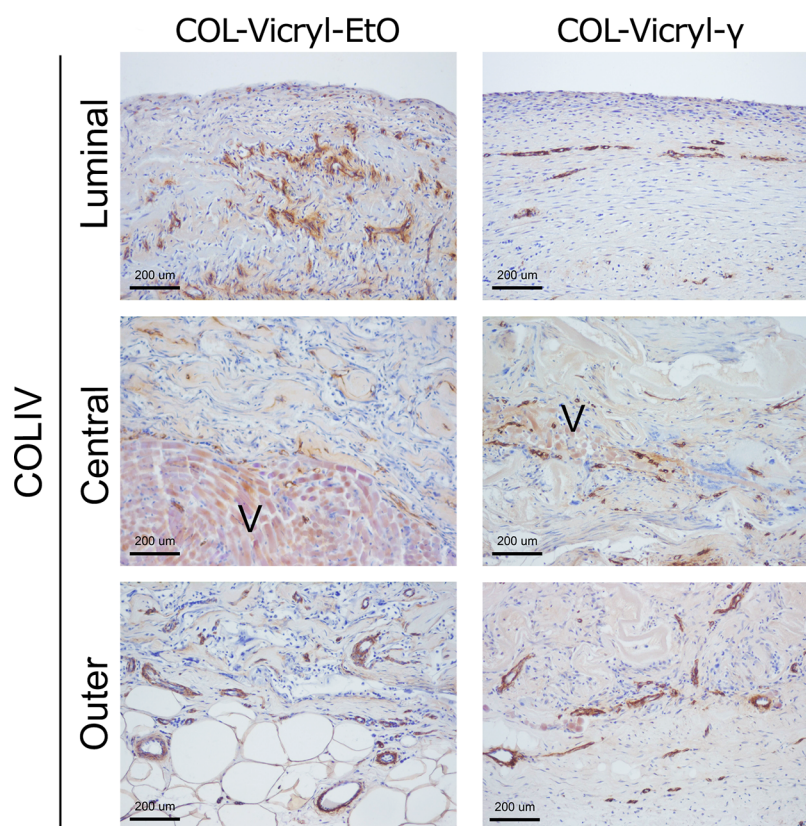


**Figure 5.** Evaluation of vascularization in COL-Vicryl-EtO and COL-Vicryl- $\gamma$  implant. Luminal, middle and outer areas of implants were stained with COLIV to visualize the vasculature. Outer and central areas are comparable between construct types. However, the luminal area showed a thin organized architecture of vasculature in the COL-Vicryl- $\gamma$ , which is comparable to native urinary tissue. The COL-Vicryl-EtO shows an aberrant vasculature in the luminal area. V = Vicryl, scale bar = 200  $\mu$ m.

shows that sterilization procedures are a crucial aspect in template design as they significantly influence tissue remodeling upon implantation. Therefore, evaluation of the effects of the sterilization procedures should become standard in early biomaterial development. Moreover, we demonstrate that *in vitro* data cannot be solely used as predictive factors for material behavior *in vivo*: whereas remodeling of EtO-sterilized constructs—the initial method of choice—was limited, enhanced tissue remodeling was observed after  $\gamma$ -sterilization. That is, the *in vivo* behavior of templates is heavily dependent on the sterilization methods used. Biomaterial evaluation, preferably in a large animal, is required to facilitate clinical translation and registration as a medical device.

In the *in vitro* part of this study, we evaluated the mechanical and morphological characteristics of the hybrid tubular constructs. For urological tissue engineering and specifically the artificial urinary conduit, the addition of a reinforcing polymer to the collagen, e.g., Vicryl, is desired to provide additional strength for template functionality and surgical handling.<sup>25,28</sup> Terminal sterilization of this hybrid tubular construct by EtO degassing or  $\gamma$ -irradiation did not lead to major differences between constructs with respect to the morphological and mechanical characteristics, similar to earlier studies for collagen alone.<sup>29</sup> Other studies already showed that  $\gamma$ -sterilization of collagen results in enhanced enzymatic degradation and reduced integrity and stability due to chain disintegration in collagen molecules in comparison to the nonsterilized construct. In contrast, the structure and stability of EtO-sterilized collagen is reported to remain unaltered and

comparable to unsterilized scaffolds.<sup>29,30</sup> The enhanced tissue remodeling of the  $\gamma$ -irradiated constructs, when placed in a subcutaneous pocket in our study, may well be explained by the  $\gamma$ -irradiation induced alterations of the collagen.

Furthermore, we assessed the influence of a wet environment using either urine, mimicking direct implantation, e.g., when used as an artificial urinary conduit, or Simulated Body Fluid (SBF), mimicking subcutaneous implantation. Interestingly, exposure of both constructs to urine resulted in immediate loss of Vicryl polymer integrity (3 days). This suggests that direct implantation of the construct in the urinary tract will lead to material collapse before sufficient tissue regeneration can occur and may therefore not be advisable. Preimplantation to form neo-tissue may solve this by creating a (semi)autologous construct.

The biomechanical properties of absorbable multifilament sutures, like Vicryl, have been previously evaluated in equine urine and similarly showed a total loss of Vicryl integrity, albeit after 21 days.<sup>31</sup> The absence of any buffering capacity of both goat and equine urine may have influenced Vicryl degradation by enhancing pH-dependent hydrolysis. The higher degradation rate of the Vicryl mesh observed in our study was probably the consequence of additional  $\gamma$ -sterilization of the commercially available and already sterilized Vicryl polymer mesh.<sup>32</sup>

Exposing the construct to SBF instead of urine prolonged Vicryl polymer stability up to 2 weeks. At this time, the strength and Young's modulus of the COL-Vicryl-EtO were significantly higher than the COL-Vicryl- $\gamma$ . After 28 days, signs



of collagen degradation (swelling) were observed in the EtO-sterilized construct and not in the  $\gamma$ -sterilized constructs. The swelling may have been the consequence of the thinner and compressed wall in the COL-Vicryl-EtO. The  $\gamma$ -sterilization results in additional cross-linking and strengthening of collagen, which may explain this difference.<sup>33</sup> In contrast, it is well established that sterilization of Vicryl by  $\gamma$ -irradiation results in enhanced degradability due to chain fragmentation.<sup>34</sup> Although this explains the lower Young's modulus of the COL-Vicryl- $\gamma$  over time, this *in vitro* assay only evaluated material degradation, while the creation of an autologous tissue tube is a balance between material degradation and tissue regeneration. Adequate assessment of this balance requires *in vivo* analysis.

Besides the slightly prolonged stability of the COL-Vicryl-EtO in a wet environment, neither of the constructs was superior in the *in vitro* analyses. Both constructs were therefore tested in a subcutaneous implantation model. Interestingly, when the implanted constructs were harvested, tissue ingrowth of preimplanted COL-Vicryl- $\gamma$  was much further developed compared to EtO-degassed constructs. In accordance with the *in vitro* data, the Vicryl polymer in the EtO-sterilized constructs was less susceptible to degradation *in vivo* and contributed to prolonged strength over time. This is in agreement with a previous study showing that  $\gamma$ -irradiation enhanced Vicryl degradation when implanted in the lumbar muscle of rats.<sup>22,33</sup> It is likely that the enhanced degradation rate of Vicryl facilitates the ingrowth of surrounding tissue and the formation of an organized subluminal vasculature in the preimplanted COL-Vicryl- $\gamma$ . The aberrant vascular architecture in the COL-Vicryl-EtO preimplant may have been the consequence of prolonged and increased levels of hypoxia. Full comprehension of the sterilization effect required functional analysis *in vivo*. Our earlier studies suggested that perhaps prolongation of template stability to achieve sustained mechanical stability might be important in the formation of the artificial conduit.<sup>17</sup> Indeed, our *in vitro* analyses showed that prolonged stability in a fluid could be accomplished by applying EtO sterilization to the hybrid tubular construct. However, the COL-Vicryl-EtO was not superior *in vivo*. Clearly, other aspects like cellular ingrowth and vascularization are equally or even more important. Furthermore, mechanical analysis after implantation did not indicate a difference in strength or elasticity, suggesting that the loss of construct integrity is compensated by tissue ingrowth, with no net loss of strength as a result.

Absorption of urine by collagen scaffolds may cause aberrant remodeling. Previously, cell seeded constructs have been tested as urostomy constructs, but this was not very successful, although urine exposure of the collagen graft was limited.<sup>20</sup> In an ongoing pilot experiment, we noticed that creation of an artificial conduit with preimplanted COL-Vicryl-EtO tubes was not successful due to disconnection from the ureter and poor integration to the surrounding tissue. In contrast, when the completely remodeled COL-Vicryl- $\gamma$  construct was used, this ultimately resulted in a functional conduit (results not shown, manuscript in preparation), showing that urine did not influence the outcome of constructs aligned with cells but that the outcome is more dependent on the sterilization method used.

EtO degassing and  $\gamma$ -irradiation are two of the most commonly used and FDA-approved sterilization techniques and were therefore chosen as comparators. Recently, novel sterilization techniques, like supercritical carbon dioxide (scCO<sub>2</sub>), have come available, and this may provide a valuable

alternative.<sup>35</sup> In combination with an altered collagen component and/or bioreactor conditioning in combination with cells, this may ultimately lead to superior constructs for *in vivo* use. Our study shows that for full comprehension of the effect of a novel sterilization method on *in vivo* biomaterial behavior, a complete panel of analyses ranging from mechanical characterization to implantation in a functional setting in a large animal model is essential.

## CONCLUSION

Thorough analysis of the *in vitro* and *in vivo* behavior of sterilized collagen-Vicryl tubular templates shows that the effect of final sterilization is considerable. Subcutaneous implantation of a  $\gamma$ -sterilized hybrid template resulted in better tissue remodeling compared to EtO-sterilized constructs. This study shows that sterilization affects tissue remodeling upon implantation. Clinical translation of tissue engineered biomaterials can only be achieved when EMA-FDA-approved sterilization methods are included in a full panel of *in vitro* and *in vivo* analyses.

## AUTHOR INFORMATION

### Corresponding Author

\*Tel.: +31(0)243610502. E-mail: [egbert.oosterwijk@radboudumc.nl](mailto:egbert.oosterwijk@radboudumc.nl)

### ORCID

Heinz P. Janke: [0000-0003-2384-7645](https://orcid.org/0000-0003-2384-7645)

### Present Addresses

<sup>§</sup>M.S.: Department of Biomedical Engineering—Faculty of Health, Medicine and Life Sciences, Maastricht University, Universiteitssingel (UNS) 50, 6229 ER Maastricht, The Netherlands. E-mail: [m.sloff@maastrichtuniversity.nl](mailto:m.sloff@maastrichtuniversity.nl)

<sup>||</sup>P.K.J.D.J.: Department of Laboratory Medicine—Laboratory of Hematology, Radboud University Medical Center, Geert Grooteplein 10, 6525 GA Nijmegen, The Netherlands. E-mail: [paul.dejonge@radboudumc.nl](mailto:paul.dejonge@radboudumc.nl)

<sup>†</sup>S.M.M.: Department of Nephrology and Hypertension—Division Internal Medicine and Dermatology, University Medical Center Utrecht, Heidelberglaan 100, 3584 CX Utrecht, The Netherlands. E-mail: [s.m.mihaila@umcutrecht.nl](mailto:s.m.mihaila@umcutrecht.nl)

### Author Contributions

<sup>#</sup>These authors contributed equally. The manuscript was written through contributions of all authors. All authors have given approval to the final version of the manuscript.

### Funding

This work was financially supported by Fonds NutsOhra (FNO), Kunststoma 1102-56 ([www.stichtingnutsohra.nl](http://www.stichtingnutsohra.nl)), and PIDON, Novio Tissue, PID 101020. Additionally, the research leading to these results has received funding from the People Programme (Marie Curie Actions) of the European Union's Seventh Framework Programme FP7/2007–2013/ under REA grant agreement no. 607868 (iTERM).

### Notes

The authors declare no competing financial interest.

## ACKNOWLEDGMENTS

C. Van den Broek, T. Wijga, A. E. J. Hanssen, and M. M. A. School (Radboudumc, Nijmegen, The Netherlands) are greatly acknowledged for their participation and assistance during the animal experiments.

## REFERENCES

- (1) Morimoto, N.; Kakudo, N.; Matsui, M.; Ogura, T.; Hara, T.; Suzuki, K.; Yamamoto, M.; Tabata, Y.; Kusumoto, K. Exploratory Clinical Trial of Combination Wound Therapy with a Gelatin Sheet and Platelet-Rich Plasma in Patients with Chronic Skin Ulcers: Study Protocol. *BMJ. Open* **2015**, *5* (5), e007733.
- (2) Omori, K.; Nakamura, T.; Kanemaru, S.; Asato, R.; Yamashita, M.; Tanaka, S.; Magruffov, A.; Ito, J.; Shimizu, Y. Regenerative Medicine of the Trachea: The First Human Case. *Ann. Otol., Rhinol., Laryngol.* **2005**, *114* (6), 429–433.
- (3) Crawford, D. C.; DeBerardino, T. M.; Williams, R. J., 3rd NeoCart, an Autologous Cartilage Tissue Implant, Compared with Microfracture for Treatment of Distal Femoral Cartilage Lesions: An FDA Phase-II Prospective, Randomized Clinical Trial after Two Years. *J. Bone Jt. Surg Am.* **2012**, *94* (11), 979–989.
- (4) Joseph, D. B.; Borer, J. G.; De Filippo, R. E.; Hodges, S. J.; McLorie, G. A. Autologous Cell Seeded Biodegradable Scaffold for Augmentation Cystoplasty: Phase II Study in Children and Adolescents with Spina Bifida. *J. Urol.* **2014**, *191* (5), 1389–1395.
- (5) Grimes, M.; Pembroke, J. T.; McGloughlin, T. The Effect of Choice of Sterilisation Method on the Biocompatibility and Biodegradability of SIS (Small Intestinal Submucosa). *Biomed Mater. Eng.* **2005**, *15* (1–2), 65–71.
- (6) Rnjak-Kovacina, J.; DesRochers, T. M.; Burke, K. A.; Kaplan, D. L. The Effect of Sterilization on Silk Fibroin Biomaterial Properties. *Macromol. Biosci.* **2015**, *15* (6), 861–874.
- (7) Watanabe, T.; Kanda, K.; Yamanami, M.; Ishibashi-Ueda, H.; Yaku, H.; Nakayama, Y. Long-Term Animal Implantation Study of Biotube-Autologous Small-Caliber Vascular Graft Fabricated by in-Body Tissue Architecture. *J. Biomed. Mater. Res., Part B* **2011**, *98* (1), 120–126.
- (8) Wang, Z.; Roberge, C.; Dao, L. H.; Wan, Y.; Shi, G.; Rouabhia, M.; Guidoin, R.; Zhang, Z. In Vivo Evaluation of a Novel Electrically Conductive Polypyrrole/Poly(D,L-Lactide) Composite and Polypyrrole-Coated Poly(D,L-Lactide-Co-Glycolide) Membranes. *J. Biomed. Mater. Res.* **2004**, *70* (1), 28–38.
- (9) Nguyen, H.; Morgan, D. A.; Forwood, M. R. Sterilization of Allograft Bone: Effects of Gamma Irradiation on Allograft Biology and Biomechanics. *Cell Tissue Bank* **2007**, *8* (2), 93–105.
- (10) Delgado, L. M.; Pandit, A.; Zeugolis, D. I. Influence of Sterilisation Methods on Collagen-Based Devices Stability and Properties. *Expert Rev. Med. Devices* **2014**, *11* (3), 305–314.
- (11) Sloff, M.; de Vries, R.; Geutjes, P.; Int'Hout, J.; Ritskes-Hoitinga, M.; Oosterwijk, E.; Feitz, W. Tissue Engineering in Animal Models for Urinary Diversion: A Systematic Review. *PLoS One* **2014**, *9* (6), e98734.
- (12) Sloff, M.; Simaioforidis, V.; de Vries, R.; Oosterwijk, E.; Feitz, W. Tissue Engineering of the Bladder—Reality or Myth? A Systematic Review. *J. Urol.* **2014**, *192* (4), 1035–1042.
- (13) Dearth, C. L.; Keane, T. J.; Carruthers, C. A.; Reing, J. E.; Huleihel, L.; Ranallo, C. A.; Kollar, E. W.; Badylak, S. F. The Effect of Terminal Sterilization on the Material Properties and in Vivo Remodeling of a Porcine Dermal Biologic Scaffold. *Acta Biomater.* **2016**, *33*, 78–87.
- (14) Matuska, A. M.; McFetridge, P. S. The Effect of Terminal Sterilization on Structural and Biophysical Properties of a Decellularized Collagen-Based Scaffold; Implications for Stem Cell Adhesion. *J. Biomed. Mater. Res., Part B* **2015**, *103* (2), 397–406.
- (15) Mendes, G. C.; Brandao, T. R.; Silva, C. L. Ethylene Oxide Sterilization of Medical Devices: A Review. *Am. J. Infect. Control* **2007**, *35* (9), 574–581.
- (16) Phillip, E., Jr.; Murthy, N. S.; Bolikal, D.; Narayanan, P.; Kohn, J.; Lavelle, L.; Bodnar, S.; Pricer, K. Ethylene Oxide's Role as a Reactive Agent during Sterilization: Effects of Polymer Composition and Device Architecture. *J. Biomed. Mater. Res., Part B* **2013**, *101* (4), 532–540.
- (17) Geutjes, P.; Roelofs, L.; Hoogenkamp, H.; Walraven, M.; Kortmann, B.; de Gier, R.; Farag, F.; Tiemessen, D.; Sloff, M.; Oosterwijk, E.; et al. Tissue Engineered Tubular Construct for Urinary Diversion in a Preclinical Porcine Model. *J. Urol.* **2012**, *188* (2), 653–660.
- (18) Abraham, G. A.; Murray, J.; Billiar, K.; Sullivan, S. J. Evaluation of the Porcine Intestinal Collagen Layer as a Biomaterial. *J. Biomed. Mater. Res.* **2000**, *51* (3), 442–452.
- (19) Rahmanian-Schwarz, A.; Held, M.; Knoeller, T.; Stachon, S.; Schmidt, T.; Schaller, H. E.; Just, L. Vivo Biocompatibility and Biodegradation of a Novel Thin and Mechanically Stable Collagen Scaffold. *J. Biomed. Mater. Res., Part A* **2014**, *102* (4), 1173–1179.
- (20) Sloff, M.; Simaioforidis, V.; Tiemessen, D. M.; Janke, H. P.; Kortmann, B. B. M.; Roelofs, L. A. J.; Geutjes, P. J.; Oosterwijk, E.; Feitz, W. F. J. Tubular Constructs as Artificial Urinary Conduits. *J. Urol.* **2016**, *196* (4), 1279–1286.
- (21) Leonhäuser, D.; Vogt, M.; Tolba, R. H.; Grosse, J. O. Potential in Two Types of Collagen Scaffolds for Urological Tissue Engineering Applications – Are There Differences in Growth Behaviour of Juvenile and Adult Vesical Cells? *J. Biomater. Appl.* **2016**, *30* (7), 961–973.
- (22) Bird, I. N.; Silver, I. A.; Gorham, S. D.; French, D. A. In Vivo Degradation of Collagen-Vicryl Materials in Rabbit Ear Chambers. *J. Mater. Sci.: Mater. Electron.* **1991**, *2* (1), 36–42.
- (23) Sloff, M.; Simaioforidis, V.; Geutjes, P. J.; Hoogenkamp, H. R.; van Kuppevelt, T. H.; Daamen, W. F.; Oosterwijk, E.; Feitz, W. F. Novel Tubular Constructs for Urinary Diversion: A Biocompatibility Study in Pigs. *J. Tissue Eng. Regen. Med.* **2017**, *11* (8), 2241–2249.
- (24) Olde Damink, L. H.; Dijkstra, P. J.; van Luyn, M. J.; van Wachem, P. B.; Nieuwenhuis, P.; Feijen, J. Cross-Linking of Dermal Sheep Collagen Using a Water-Soluble Carbodiimide. *Biomaterials* **1996**, *17* (8), 765–773.
- (25) Janke, H. P.; Bohlin, J.; Lomme, R. M. L. M.; Mihaila, S. M.; Hilborn, J.; Feitz, W. F. J.; Oosterwijk, E. Bioinspired Coupled Helical Coils for Soft Tissue Engineering of Tubular Structures – Improved Mechanical Behavior of Tubular Collagen Type I Templates. *Acta Biomater.* **2017**, *59*, 234–242.
- (26) Lin, C.-H.; Kao, Y.-C.; Lin, Y.-H.; Ma, H.; Tsay, R.-Y. A Fiber-Progressive-Engagement Model to Evaluate the Composition, Microstructure, and Nonlinear Pseudoelastic Behavior of Porcine Arteries and Decellularized Derivatives. *Acta Biomater.* **2016**, *46*, 101–111.
- (27) Oyane, A.; Kim, H. M.; Furuya, T.; Kokubo, T.; Miyazaki, T.; Nakamura, T. Preparation and Assessment of Revised Simulated Body Fluids. *J. Biomed. Mater. Res.* **2003**, *65* (2), 188–195.
- (28) Hoogenkamp, H. R.; Koens, M. J. W.; Geutjes, P. J.; Ainoedhofer, H.; Wanten, G.; Tiemessen, D. M.; Hilborn, J.; Gupta, B.; Feitz, W. F. J.; Daamen, W. F.; et al. Seamless Vascularized Large-Diameter Tubular Collagen Scaffolds Reinforced with Polymer Knittings for Esophageal Regenerative Medicine. *Tissue Eng., Part C* **2014**, *20* (5), 423–430.
- (29) Faraj, K. A.; Brouwer, K. M.; Geutjes, P. J.; Versteeg, E. M.; Wismans, R. G.; Deprest, J. A.; Chajra, H.; Tiemessen, D. M.; Feitz, W. F. J.; Oosterwijk, E. The Effect of Ethylene Oxide Sterilisation, Beta Irradiation and Gamma Irradiation on Collagen Fibril-Based Scaffolds. *Tissue Eng. Regen. Med.* **2011**, *8* (5), 460–470.
- (30) Noah, E. M.; Chen, J.; Jiao, X.; Heschel, I.; Pallua, N. Impact of Sterilization on the Porous Design and Cell Behavior in Collagen Sponges Prepared for Tissue Engineering. *Biomaterials* **2002**, *23* (14), 2855–2861.
- (31) Kearney, C. M.; Buckley, C. T.; Jenner, F.; Moissonnier, P.; Brama, P. A. Elasticity and Breaking Strength of Synthetic Suture Materials Incubated in Various Equine Physiological and Pathological Solutions. *Equine Vet J.* **2014**, *46* (4), 494–498.
- (32) Kerstein, R. L.; Sedaghati, T.; Seifalian, A. M.; Kang, N. Effect of Human Urine on the Tensile Strength of Sutures Used for Hypospadias Surgery. *J. Plast Reconstr Aesthet Surg* **2013**, *66* (6), 835–838.
- (33) Gorham, S. D.; Srivastava, S.; French, D. A.; Scott, R. The Effect of Gamma-Ray and Ethylene Oxide Sterilization on Collagen-Based Wound-Repair Materials. *J. Mater. Sci.: Mater. Med.* **1993**, *4* (1), 40–49.



(34) Chu, C. C.; Williams, D. F. The Effect of Gamma Irradiation on the Enzymatic Degradation of Polyglycolic Acid Absorbable Sutures. *J. Biomed. Mater. Res.* **1983**, *17* (6), 1029–1040.

(35) Balestrini, J. L.; Liu, A.; Gard, A. L.; Huie, J.; Blatt, K. M.; Schwan, J.; Zhao, L.; Broekelmann, T. J.; Mecham, R. P.; Wilcox, E. C.; et al. Sterilization of Lung Matrices by Supercritical Carbon Dioxide. *Tissue Eng., Part C* **2016**, *22* (3), 260–9.